Hindawi
Scientific Programming
Volume 2022, Article ID 1319087, 8 pages
https://doi.org/10.1155/2022/1319087

Research Article

Dimensionality Reduction and Extraction of Engineering Remote Sensing Data Based on Building Information Modeling and Geographical Information System

Yonghua Wang,[1] **Yanfang Li**,[1] **Bing Zhang**,[1] **and Pengxiang Xing**[2]

[1]*College of Civil Engineering, Tangshan University, Tangshan 063000, China*
[2]*China Railway 15th Bureau Group Co., Ltd., Shanghai 510632, China*

Correspondence should be addressed to Yonghua Wang; tscwyh@tsc.edu.cn

Received 18 March 2022; Revised 18 April 2022; Accepted 28 April 2022; Published 11 May 2022

Academic Editor: Sheng Bin

The high dimensionality of the modern remote sensing data of construction land makes it complicated to extract image data. This paper proposes a dimensionality reduction and extraction strategy for the remote sensing data of construction land, with the aid of building information modeling (BIM) and geographical information system (GIS). Firstly, the BIM was employed to reduce the size of the remote sensing data of construction land and to obtain the information of each element. Next, the remote sensing data of construction land were parsed, and the key BIM elements were extracted through semantic filtering. In addition, the remote sensing data were converted into a triangulated irregular network (TIN), which can be processed by the geographical information system (GIS). In the end, random projection was utilized to reduce the dimensionality and compress the remote sensing data, and realize the data extraction. Experimental results show that our approach can compress and extract the information from construction land images in the remote sensing data with a high accuracy.

1. Introduction

With the rapid development of society, urban construction requires better management, standardization, refinement, scientific planning, and low-carbon environmental protection development. This poses a huge challenge to scientific research and engineering technology. It is impossible to satisfy the high requirements of construction land date and information with a single technical means.

In recent years, building information modeling (BIM) has developed quickly as a technique applicable to construction and related industries [1–3]. The technique boasts rich and consistent semantic information, as well as refined geometric structure. For example, BIM can integrate the information of each stage of engineering construction into the BIM model and display the detail information of buildings through the model. It is in line with the goal of refined management of urban buildings. The BIM can realize the intelligence and collaboration of building management, support the real-time sharing of massive data in buildings [4, 5], and meet the various requirements of building planning and approval.

Three-dimensional (3D) geographical information system (GIS) is an important technique to combine and display the spatial structure of buildings and the terrain. The technique facilitates the micro and macro management of multiscale data of buildings and provides technical support for the approval and investigation of construction land [6–8].

The information related to urban construction land can be exchanged through multiple fields. The multifield information exchange is an important aspect of information sharing and collaboration in the development and construction of smart cities. The urban construction land can be presented in digital form using the BIM [9] to thoroughly display the rich semantic information of the construction land, including physical properties, geometry, and regularity.

Remote sensing images are featured by rich information, complex features, and clear details. Feature compression and extraction is an important way to analyze massive remote sensing data [10]. As a spatial database technique, the GIS can store a huge amount of 3D spatial data and manage and visualize the massive data effectively [11, 12]. Thus, it plays an important role in the management and analysis of urban construction land. Remote sensing images and data are the main information sources and core components of the GIS. With the aid of the GIS, it is possible to effectively analyze and manage spatial data, and enhance the utilization value of images and data [13].

Under the BIM, this paper proposes a dimensionality reduction and extraction approach for remote sensing data of construction land. The BIM was adopted to process a massive amount of urban construction land. The processed data were converted into the GIS software. Experimental results show that the data on urban construction land were effectively extracted through our approach of dimensionality reduction and extraction. The extracted construction land data can be used to support urban renewal and transformation planning, land acquisition planning, construction land approval, economic and social development planning, digital city (smart city) construction, etc.

2. Methodology

2.1. Flow. The BIM was applied to construction land, aiming to support building planning and approval with complete and accurate data. Specifically, the BIM was integrated with the GIS [14–18]. The collected remote sensing data were parsed by the BIM and compressed to extract urban construction land. The flow of the compression and extraction scheme of urban construction land is explained as follows (see Figure 1):

The target data are imported to the BIM model. The data size is reduced to obtain the element information required for construction land. After a thorough analysis on the data of construction land, the key elements of the BIM are extracted, and the postextraction data are converted to the GIS model. Then, the remote sensing data are dimensionally reduced through random projection and extracted with the aid of visual word graph.

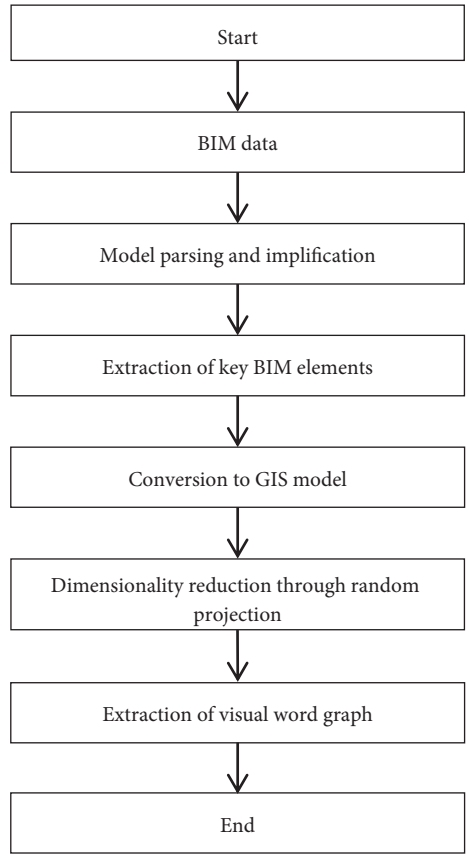

Figure 1: Flow of data compression and extraction.

2.2. Key Element Extraction and Data Conversion. The BIM involves building settings and spatial interfaces, which cover the whole process from building design, construction, to management. Depending on the different research directions, the BIM model was simplified and used to process the remote sensing data. After filtering the relevant information, the key elements of construction land were obtained. Figure 2 shows the flow of key element extraction and data conversion.

In the past, the application of BIM to construction land extraction has the disadvantage of data redundancy, which complicates the construction land approval [19]. Here, semantic filtering is implemented according to the specific requirements of construction land, before extracting the land. Different data filter banks were adopted to filter out the redundant semantics of construction land [20].

In remote sensing images, the main land uses include high-density construction areas, low-density construction areas, new construction areas, mountains, forests, shrubs, farmlands, lakes, seas, and rivers. According to the type of the construction land, the words irrelevant to the construction land were selected as semantic filter banks, such as mountains, forests, shrubs, farmlands, lakes, seas, and rivers. Only the semantics related to construction land were preserved.

Next, the internal elements of the BIM model were combined with the constraints of semantic filter banks to obtain the key information from the semantic filter banks. After that, the BIM entity model was converted into a triangulated irregular network (TIN), which can be processed by the GIS. During the conversion, the coordinate conversion matrix of the GIS model was obtained, and the contours of construction land were mapped to the global coordinate system of the GIS model.

The identity (ID) value was employed to provide data, including the semantic information and geometric information related to construction land, for data management of the GIS model. The BIM relies on coordinates to locate construction land. When massive data were imported to the GIS model, the specific coordinates were determined by comparing each Revit measuring point with actual measuring point. In this way, the construction land, which is

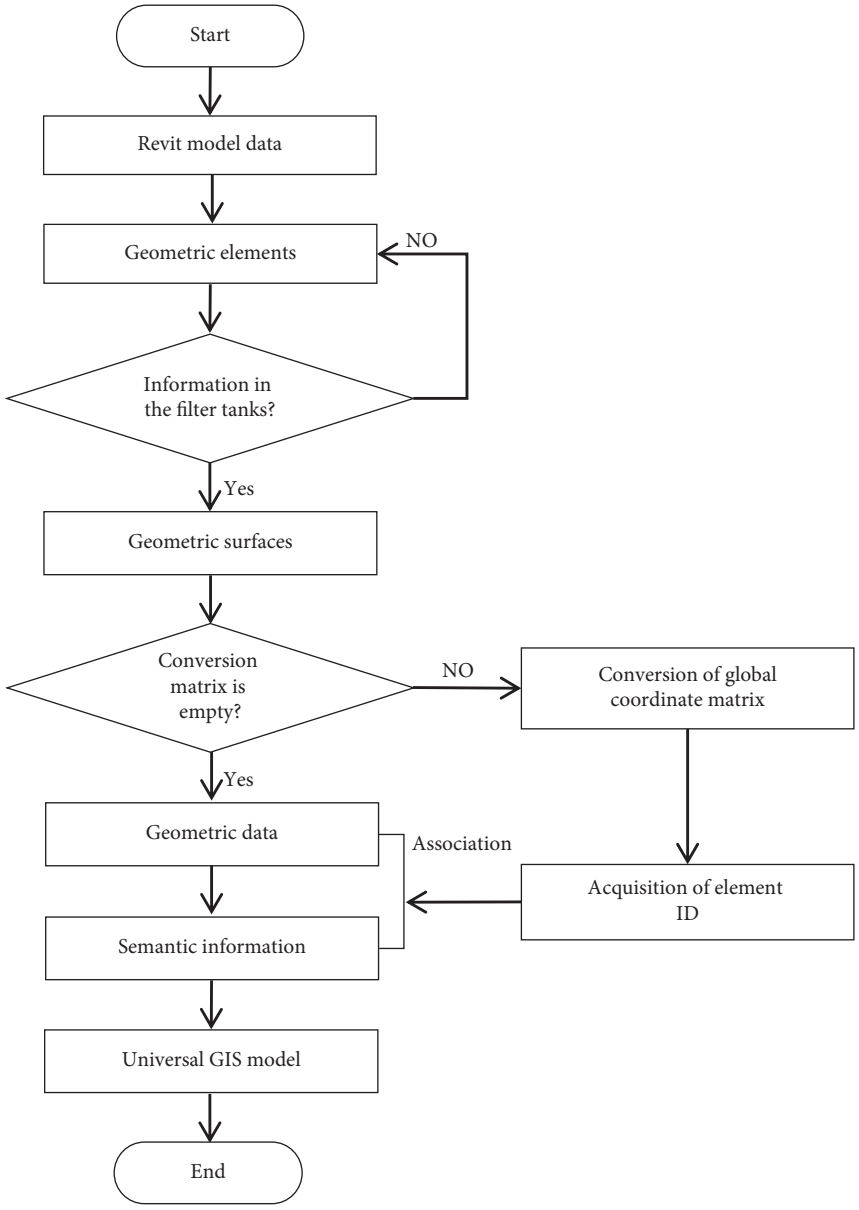

Figure 2: Flow of key element extraction and data conversion.

extracted from massive remote sensing data after being compressed by the BIM, can be converted to the correct positions in the GIS model coordinate system.

2.3. Dimensionality Reduction and Extraction. The dimensionality reduction and extraction of remote sensing data consists of two parts: dimensionality reduction and feature extraction. The former was realized through random projection, and the latter was achieved with the aid of visual word graph.

2.3.1. Dimensionality Reduction. Let I be a remote sensing image containing n wave bands; $b \times b$ be the size of the image window extracted from each band of the image according to the ranking of pixels. The pixels can be ranked by the following rule:

$$z^{S_q} = \left[q_{0,0} \ \ \mathrm{sort}\left(q_{1,0}, \cdots, q_{1,t_1}\right) \ \cdots \ \mathrm{sort}\left(q_{a,0}, \cdots, q_{1,t_a}\right) \right]^T, \tag{1}$$

where $q0.0$ is the central pixel; $a = 1, 2, \cdots, \mathrm{fix}\,(b/2)$.

All the grayscale values on the rectangular ring centering on the $b \times b$ window are ranked by formula (1). After ranking, these values are connected in series to form the original eigenvector $z^{S_q} \in W^{b^2}$.

Then, spatial information is integrated with the spectrum, and the eigenvector containing n bands are prepared into a new eigenvector $z^{S_q} \in W^{nb^2 \times 1}$:

$$Z^{CS} = \Gamma z^{S_q}, \tag{2}$$

where $\Gamma \in W^{h \times k}$ is the random projection matrix, with $k = nb^2$ and $h \ll k$. The subspace of compressed features $\{Z^{CS}\}$ encompasses all compressed eigenvectors.

The size parameter of the random projection matrix Γ should conform to the Johnson–Lindenstrauss (JL) lemma. According to the compressed sensing theory, this parameter must have the restricted isometry property.

2.3.2. Feature Extraction Based on Visual Word Graph. In the visual word graph, the texture primitives are defined as the central words at all pixels and the words in the $u \times u$ neighborhood of each pixel. Here, the visual word graph is utilized to extract the construction land from the original remote sensing image and treat it as the texture feature of the pixel of interest. The texture information-containing texture primitives thus obtained are of the size $b \times b$. They can reflect the properties of texture primitives with high quality [21]. In the visual word graph, the words in the $u \times u$ neighborhood manifest the global spatial information, as well as the spatial information of the class of each central pixel. The multiscale remote sensing data can be illustrated by reflecting the problem features with two windows. With the aid of visual word graph, the global texture features of construction land can be extracted in three steps: dictionary learning, word encoding, and feature extraction.

(1) Dictionary learning.

The k-means clustering (KMC) is applied to compress the feature subspace. With Euclidean distance as the similarity metric, the training samples $\{Z_{T_i}^{CS}\}$ are clustered. The cluster center is the dictionary s_i of the corresponding cluster.

Let C and K be the number of sample classes and the number of cluster centers, respectively. From the different types of dictionaries, the final compressed texture dictionary $S \in W^{h \times CK} = \{s_1, s_2, \cdots, s_C\}$ can be obtained, with the size of CK.

(2) Word encoding.

The texture dictionary S is established by the e nearest neighbor algorithm. Then, the Euclidean distance from each word in S to the texture primitives in S is computed, and each texture primitive is numbered with the code of the nearest word. Next, the codes of the words in the $u \times u$ neighborhood and the central words are compiled into the texture primitive $l_{i,j}$ corresponding to each word in the visual word graph, with the central pixel being denoted as $x_{0,0}$.

(3) Feature extraction.

The statistical features of the remote sensing data are represented by the word histogram $G = [\eta_1 \ \eta_2 \ \cdots \ \eta_{CK}]^T$ of the visual word graph, where η_i is the number of appearances of word i in the visual word graph. The spatial information of words in the visual word graph is added to improve the extraction accuracy [22]. The spatial distribution information in the graph is represented by the second-order moments $R = [\mu_1 \ \mu_2 \ \cdots \ \mu_{CK}]^T$ of different words relative to the central pixel, where $\mu_i = \sum_{j=1}^{\eta_i} (s_{i,j} - \bar{s}_i)^2 / \eta_i$, with $s_{i,j}$ and $\bar{s}_i$ being the distance to the central pixel and the mean distance to the central pixel, respectively.

Figure 3: Original remote sensing image.

Figure 4: Extracted construction land.

The second-order moment information and histogram information are fused to obtain the final texture metric $Z \in W^{2CK \times 1}$:

$$Z = (G; R). \tag{3}$$

3. Experiments and Result Analysis

3.1. Experimental Plan. This section intends to verify the effectiveness of the proposed BIM-based approach for dimensionality reduction and extraction of remote sensing data of construction land. The region in the east of Dazu District, Chongqing, China was selected as the experimental area. The proposed approach was programmed in Java on a computer running on Windows XP. Figure 3 shows the original remote sensing image of the experimental area.

3.2. Result Analysis. Figure 4 shows the construction land extracted from the original remote sensing image by the proposed approach. It can be seen that our approach can

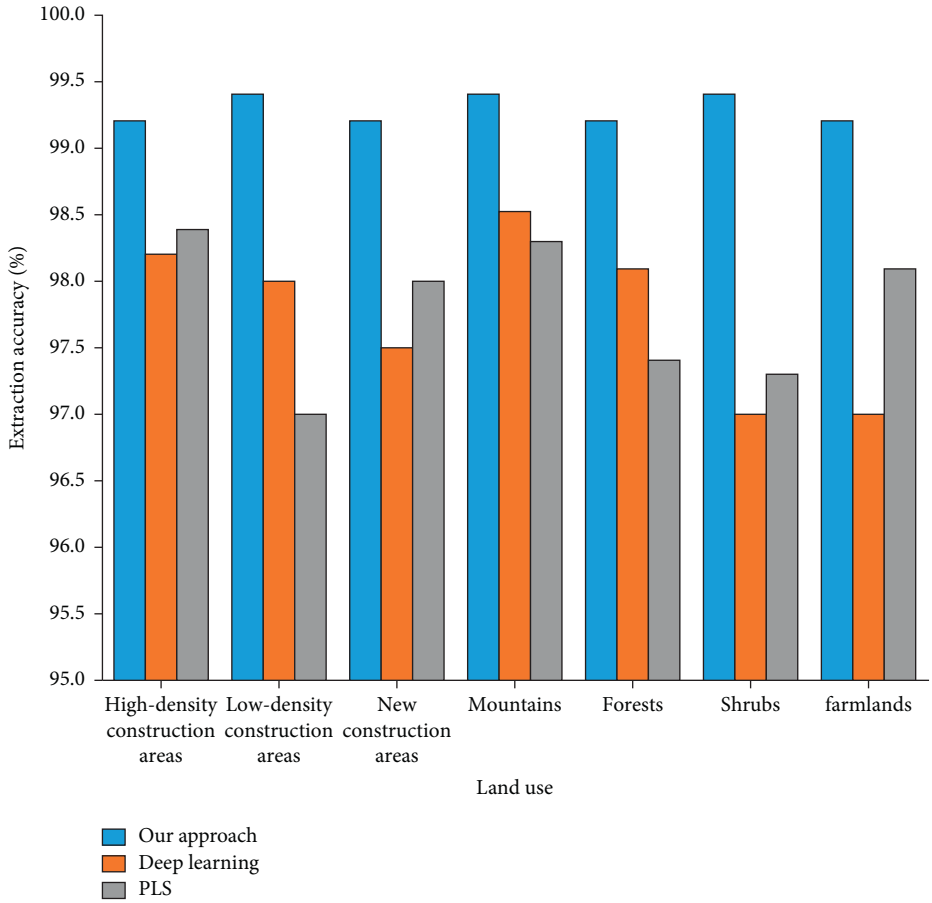

Figure 5: Extraction accuracy on each land use.

effectively extract and compress the construction land in the remote sensing image.

As shown in Figure 3, the experimental region mainly covers seven land uses: high-density construction areas, low-density construction areas, new construction areas, mountains, forests, shrubs, and farmlands. In total, there are three kinds of construction land, and four kinds of nonconstruction land. The extraction accuracy of our approach on each land use was tested to verify its effectiveness in compression and extraction. In addition, our approach was compared with deep learning and partial least square (PLS) regression (Figure 5). It can be observed that our approach extracted different land uses with an accuracy greater than 99%, much higher than that (<98.5%) of deep learning and PLS.

In the remote sensing image, the buildings are mainly multistory residential buildings, factory buildings, public buildings, single-story new houses, single-story old houses, and high-rise residential buildings. The above three approaches were separately adopted to extract the six kinds of buildings, and the number of extracted buildings was compared with the actual number of buildings (Table 1). The comparison shows that the number of buildings extracted by our approach was very close to the actual number, while that by deep learning and PLS was far from the actual number. Again, our approach was found to be highly accurate in extraction.

Next, eight buildings were randomly selected from the remote sensing image. The above three approaches were separately adopted to extract the mean circumference ratio and mean area ratio of each building. The extraction results in Figure 6 show that the construction land extracted by our approach had a much greater mean circumference ratio and mean area ratio that extracted by deep learning and PLS. Hence, our approach can extract the details of construction land with a high accuracy.

Furthermore, 10 areas were randomly selected from the remote sensing image. The above three approaches were separately adopted to extract the buildings from each area. The two errors of each approach were counted: mistaking building for nonbuilding (BFNB) and mistaking nonbuilding for building (NBFB). The results in Table 2 show that our approach had much smaller BFNB and NBFB than deep learning and PLS, evidence to the high extraction accuracy of our approach for construction land.

Table 1: Extraction accuracies of different approaches.

Building type	Actual number	Our approach	Deep learning	PLS
Multi-story residential buildings	584	582	578	581
Factory buildings	625	623	621	619
Public buildings	715	710	706	708
Single-story new houses	642	640	634	628
Single-story old houses	584	581	574	564
High-rise residential buildings	602	599	586	589
Total number	3752	3735	3699	3689

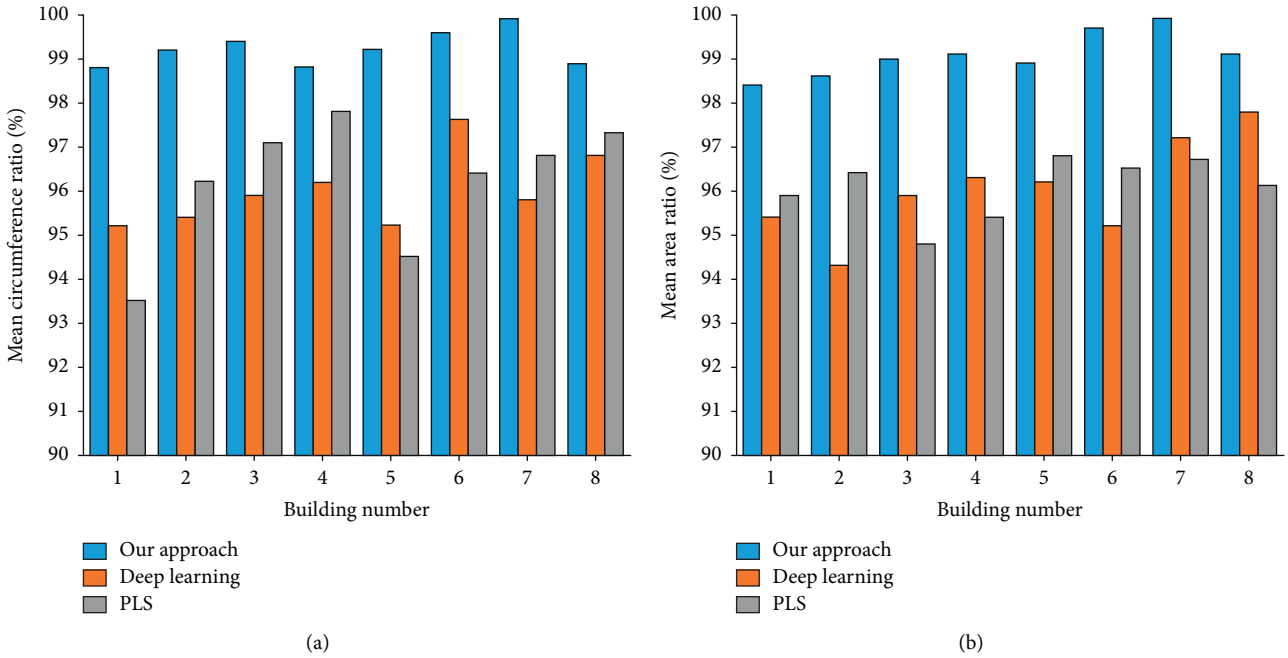

Figure 6: Comparison of mean circumference ratio and mean area ratio. (a) Mean circumference ratio. (b) Mean area ratio.

Table 2: Errors of different approaches.

Areas	Our approach		Deep learning		PLS	
	BFNB	NBFB	BFNB	NBFB	BFNB	NBFB
1	0	1	3	5	2	4
2	0	2	2	2	5	2
3	0	1	3	4	3	3
4	1	0	1	3	4	5
5	0	1	3	6	2	4
6	0	0	2	4	1	2
7	1	0	3	8	5	3
8	0	1	4	5	0	5
9	0	0	2	1	3	1
10	0	0	3	3	2	3
Total number	2	6	26	41	27	32

Finally, the above three approaches were separately adopted for feature extraction of the original remote sensing image seven times. The single-to-noise ratios (SNRs) of the construction land extracted by each approach were counted. The results in Figure 7 show that the construction land extracted by our approach from the remote sensing image had much higher SNRs than that extracted by deep learning and PLS. This means our approach can compress and extract construction land, while preserving the useful information in the image. After being processed by our approach, the images maintained high SNRs, which demonstrate the high extraction performance of our approach.

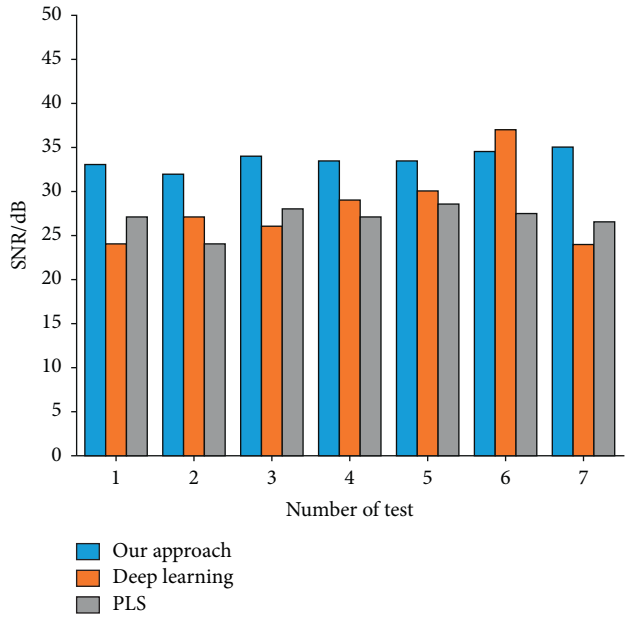

Figure 7: SNRs of results extracted by different approaches.

4. Conclusions

This paper applies the BIM to compress and extract the remote sensing data of construction land. After analyzing the necessary component information of the BIM, the authors filtered out the information unrelated to construction land and extracted construction land features through random projection and visual word graph. In this research, the data completeness of the BIM is fully utilized to maximize the extraction accuracy of construction land and to provide a technical basis for the planning and approval of urban buildings. Experimental results show that our approach can extract features at ease and differentiate between ground objects effectively.

Data Availability

The data used to support the findings of this study are available from the corresponding author upon request.

Conflicts of Interest

The authors declare that they have no conflicts of interest.

References

[1] Q.-J. Wen, Z.-J. Ren, H. Lu, and J.-F. Wu, "The progress and trend of BIM research: a bibliometrics-based visualization analysis," *Automation in Construction*, vol. 124, no. 22, Article ID 103558, 2021.

[2] Z. Peng, "An operation and maintenance strategy of intelligent building information model data based on cloud computing," *Ingénierie des Systèmes d'Information*, vol. 25, no. 4, pp. 461–467, 2020.

[3] H. Lindblad and J. R. Guerrero, "Client's role in promoting BIM implementation and innovation in construction," *Construction Management & Economics*, vol. 38, no. 5, pp. 468–482, 2020.

[4] S. Shirowzhan, S. M. E. Sepasgozar, D. J. Edwards, H. Li, and C. Wang, "BIM compatibility and its differentiation with interoperability challenges as an innovation factor," *Automation in Construction*, vol. 112, no. 11, pp. 103086–103094, 2020.

[5] H. Sözer, H. Sözen, and D. Utkucu, "Waste potential of a building through gate-to-grave approach based on life cycle assessment (LCA)," *International Journal of Sustainable Development and Planning*, vol. 15, no. 2, pp. 165–171, 2020.

[6] M. Marzouk and A. Othman, "Planning utility infrastructure requirements for smart cities using the integration between BIM and GIS," *Sustainable Cities and Society*, vol. 57, no. 16, pp. 102120–102127, 2020.

[7] N. Fareed and K. Rehman, "Integration of remote sensing and GIS to extract plantation rows from A drone-based image point cloud digital surface model," *ISPRS International Journal of Geo-Information*, vol. 9, no. 3, pp. 151–157, 2020.

[8] H. Wu and T. Song, "An evaluation of landslide susceptibility using probability statistic modeling and GIS's spatial clustering analysis," *Human and Ecological Risk Assessment: An International Journal*, vol. 24, no. 7, pp. 1952–1968, 2018.

[9] H. P. Wu and S. C. Huang, "Experimental research on information extraction of new construction land based on in-depth learning -- innovation exploration of national land use remote sensing monitoring project," *Remote Sensing of Land and Resources*, vol. 31, no. 4, pp. 159–166, 2019.

[10] M. Mahdianpari, S. Homayouni, and S. Foucher, "CJRS' special issue on deep learning for environmental applications of remote sensing data," *Canadian Journal of Remote Sensing*, vol. 47, no. 2, pp. 159–161, 2021.

[11] E. Hermas, A. Gaber, and M. El Bastawesy, "Application of remote sensing and GIS for assessing and proposing mitigation measures in flood-affected urban areas, Egypt," *The Egyptian Journal of Remote Sensing and Space Science*, vol. 24, no. 1, pp. 119–130, 2021.

[12] Q. Bi, M. Lai, H. Tang et al., "Precise inspection of geometric parameters for polyvinyl chloride pipe section based on computer vision," *Traitement du Signal*, vol. 38, no. 6, pp. 1647–1655, 2021.

[13] A. S. Muneer, K. N. Sayl, and A. H. Kamel, "Modeling of runoff in the arid regions using remote sensing and geographic information system (GIS)," *International Journal of Design & Nature and Ecodynamics*, vol. 15, no. 5, pp. 691–700, 2020.

[14] M. Marzouk and A. Othman, "Planning utility infrastructure requirements for smart cities using the integration between BIM and GIS," *Sustainable Cities and Society*, vol. 57, p. 102120, 2020.

[15] T. W. Kang and C. H. Hong, "A study on software architecture for effective BIM/GIS-based facility management data integration," *Automation in Construction*, vol. 54, pp. 25–38, 2015.

[16] J. Zhu and P. Wu, "Towards effective BIM/GIS data integration for smart city by integrating computer graphics technique," *Remote Sensing*, vol. 13, no. 10, pp. 1889–1910, 2021.

[17] D. Shkundalov and T. Vilutienė, "Bibliometric analysis of building information modeling, geographic information systems and web environment integration," *Automation in Construction*, vol. 128, Article ID 103757, 2021.

[18] G. Celeste, M. Lazoi, M. Mangia, and G. Mangialardi, "Innovating the construction life cycle through BIM/GIS

integration: a review," *Sustainability*, vol. 14, no. 2, pp. 766–773, 2022.
[19] A. Mahmood and S. Abrishami, "BIM for lean building surveying services," *Construction Innovation*, vol. 20, no. 3, pp. 447–470, 2020.
[20] H. Huang, G. Y. Shi, and Y. Duan, "Dimension reduction method of hyperspectral remote sensing image embedded by weighted space spectrum joint preservation," *Journal of Surveying and Mapping*, vol. 48, no. 8, pp. 1014–1024, 2019.
[21] J.-P. Kahane, "Compressed sensing from a harmonic analysis point of view," *Analysis Mathematica*, vol. 42, no. 1, pp. 19–29, 2016.
[22] K. S. Arun, V. K. Govindan, and S. D. M. Kumar, "Enhanced bag of visual words representations for content based image retrieval: a comparative study," *Artificial Intelligence Review*, vol. 53, no. 3, pp. 1615–1653, 2020.